The miRNA–mRNA regulatory networks of the response to NaHCO$_3$ stress in industrial hemp (*Cannabis sativa* L.)

Kun Cao[1,2], Yufeng Sun[1], Xiaoyan Zhang[1], Yue Zhao[1], Jing Bian[1], Hao Zhu[1], Pan Wang[1], Baochang Gao[1], Xiaoli Sun[2,3,4], Ming Hu[1], Yongxia Guo[2,3,4*] and Xiaonan Wang[1*]

Abstract

Background Industrial hemp is an important industrial crop and has strong resistance to saline-alkaline stress. However, research on the industrial hemp response to NaHCO$_3$ stress is limited. Therefore, the response mechanisms of industrial hemp under NaHCO$_3$ stress were analysed through miRNA–mRNA regulatory networks.

Results Seedlings of two salt–alkali tolerant and sensitive varieties were cultured in a solution containing 100 mM NaHCO$_3$ and randomly sampled at 0, 6, 12, and 24 h. With prolonged NaHCO$_3$ stress, the seedlings gradually withered, and the contents of jasmonic acid, lignin, trehalose, soluble protein, peroxidase, and superoxide dismutase in the roots increased significantly. The abscisic acid content decreased and then gradually increased. Overall, 18,215 mRNAs and 74 miRNAs were identified as differentially expressed under NaHCO$_3$ stress. The network showed that 230 miRNA–mRNA interactions involved 16 miRNAs and 179 mRNAs, including some key hub novel mRNAs of these crucial pathways. Carbon metabolism, starch, sucrose metabolism, plant hormone signal transduction, and the spliceosome (SPL) were crucial pathways in industrial hemp's response to NaHCO$_3$ stress.

Conclusions It is speculated that industrial hemp can regulate SPL pathway by upregulating miRNAs such as novel_miR_179 and novel_miR_75, thus affecting starch and sucrose metabolism, plant hormone signal transduction and carbon metabolism and improving key physiological indices such as jasmonic acid content, trehalose content, and peroxidase and superoxide dismutase activities under NaHCO$_3$ stress.

Keywords NaHCO$_3$, Industrial hemp, miRNA–mRNA regulatory networks

*Correspondence:
Yongxia Guo
gyxia@163.com
Xiaonan Wang
wxn_fern@163.com
[1] Daqing Branch of Heilongjiang Academy of Sciences, Daqing 163319, Heilongjiang, China
[2] Heilongjiang BaYi Agricultural University, Daqing 163319, Heilongjiang, China
[3] National Coarse Cereal Engineering Research Center, Daqing 163319, Heilongjiang, China
[4] Heilongjaing Province Cultivating Collaborative Innovation Center for The Beidahuang Modern Agricultural Industry Technology, Daqing 163319, Heilongjiang, China

Background

Cannabis sativa L., belonging to the family Cannabaceae, is used in industries at a tetrahydrocannabinol (THC) concentration of less than 0.3%, mainly for fibre, food, and medicine, and has great economic value [1, 2]. Heilongjiang province is one of the largest planting bases of industrial hemp. In 2017, local drug control laws were amended in Heilongjiang province, China, to regulate industrial hemp use [3].

Soil salinization is a critical factor limiting the normal growth and development of plants [4, 5]. The root and leaf surface areas and amount of dry matter mainly

Cao *et al. BMC Plant Biology*   (2023) 23:509

Page 2 of 11

represent the plant response to salt-alkali stress [6]. Plants alter their osmotic regulatory substances and antioxidant enzyme activities to grow adequately under salt-alkali stress [5, 7, 8].

Salt–alkali stress alters the expression of related resistance genes involved in oxidative stress [9], osmotic regulation [10], hormone signal transduction [11], and ion homeostasis [12]. Seed germination is stimulated under a low concentration of neutral salt [2]. The saline-alkaline tolerance of various industrial hemp cultivars was compared owing to their different physiological indices [13]. Furthermore, some studies have revealed the molecular mechanisms of response to salt stress in industrial hemp [14, 15].

Highly conserved plant microRNAs (miRNAs) of approximately 22 nucleotides in length are small interfering RNA molecules that emerge as important gene expression regulators under stress [16, 17]. miRNAs regulate the gene transcription levels of target mRNAs in a sequence-specific manner [17, 18]. Additionally, miRNAs play an important role in enhancing plant tolerance against abiotic factors through negative or positive regulators approving amassing of positive regulators [19]. However, miRNAs and their molecular responses in industrial hemp under $NaHCO_3$ stress have not been well studied. In this study, we aimed to identify differentially expressed genes (DEGs) and investigate the pathways associated with $NaHCO_3$ stress. Seedling roots of 'Huoma No. 1' (salt-alkali-tolerant variety) and 'Jindao-15' (salt-alkali-sensitive variety) were used to perform miRNA–mRNA integrated analysis to explore the biological functions and the molecular mechanisms of industrial hemp response to $NaHCO_3$ stress. In summary, these findings provide numerous candidate miRNAs and mRNAs for the innovation of industrial hemp salt-tolerant germplasm resources and the cultivation of saline-alkaline-tolerant varieties. Finally, this study may improve the resistance of industrial hemp, reduce the planting costs and increase the economic benefit.

Methods
Industrial hemp and $NaHCO_3$ stress
Seeds of 'Huoma No. 1' (H) and 'Jindao-15' (J) were used as the experimental materials. The industrial hemp seeds were sterilized, germinated, and transplanted into lightproof boxes. The seedlings (three-leaf stage) were exposed to 100 mM $NaHCO_3$. The root samples were randomly sampled under $NaHCO_3$ stress for 0 h(H0, J0), 6 h(H6, J6), 12 h(H12, J12), and 24 h(H24, J24). Then, the samples were frozen in liquid nitrogen and stored at −80 ℃. Each treatment was replicated three times [15]. The physiological indices of abscisic acid (ABA) and jasmonic acid (JA) were analysed using high-performance liquid chromatography (HPLC). The contents of lignin, trehalose, soluble protein, β-amylase, peroxidase (POD), and superoxide dismutase (SOD) were analysed using an enzyme-linked immunosorbent assay (ELISA). The assay kits were provided by Suzhou Mcy Bio-pharm Technology Co., Ltd. (Suzhou, China).

Transcriptome analysis
Total RNA was extracted using TRIzol (Invitrogen, Carlsbad, CA, USA), and its concentration and integrity were determined using a Nanodrop 5000 (Thermo Fisher Scientific, Waltham, MA, USA) and Agilent 2100 (Agilent Technologies, Santa Clara, CA, USA). The miRNA was ligated to the 3′ SR and 5′ SR adaptors and reverse transcribed to create the first cDNA chain. Then, miRNA libraries were constructed using polymerase chain reaction (PCR) amplification and rubber cutting recycling of polyacrylamide gel electrophoresis (PAGE). Then, the constructed libraries were sequenced on an Illumina platform by Biomarker Technology [15]. DEGs were compared between J0 vs J12 and H0 vs H12. DEG analysis (mRNA with false discovery rate (FDR)< 0.01, fold change values ≥ 2; miRNA with P value≤0.05, fold change≥ 1.5), Gene Ontology (GO) team analysis (P value < 0.01), and Kyoto Encyclopedia of Genes and Genomes (KEGG) pathway analysis were conducted [20]. The protein–protein interaction (PPI) network was analyzed using the STRING database (http://string-db.org/) and Cytoscape [15, 21, 22]. The original miRNA and mRNA sequencing data have been submitted to NCBI under accession numbers PRJNA 813212 and PRJNA 874321.

miRNA target gene prediction and miRNA–mRNA integrated analysis
The miRNA target genes, derived from the DEGs in the industrial hemp samples, were predicted using TargetFinder software. Then, the miRNAs and their target genes were estimated, and an miRNA–mRNA integrated analysis was visualized using Cytoscape.

Quantitative real-time PCR (qRT-PCR)
Ten mRNAs and two miRNAs were selected for qRT–PCR to verify the reliability of RNA-seq. The qRT–PCR primers are listed in Supplementary Table A2. The Fast-King RT Kit (Tiangen Biotech Co., Ltd., Beijing, China) was used for reverse transcription, and Power qPCR PreMix(GeneCopoeia, Inc., Rockville, MD, USA) was used for qRT–PCR. Each sample was normalized using *GAPDH* and *U6* as internal controls and performed in triplicate [15, 23].

Cao *et al. BMC Plant Biology*   (2023) 23:509

Page 3 of 11

Results

Morphological and physiological characteristics of industrial hemp seedlings under NaHCO₃ stress

After 6 h of NaHCO₃ stress, the industrial hemp seedlings grew adequately. However, the fibrous roots were slightly yellow in colour compared with those before stress. After 12 h, root yellowing became more severe.

After 24 h, the seedlings were wilting, and the wilting of Jindao-15 (Fig. 1B) was more severe than that of Huoma No. 1 (Fig. 1A). The contents of JA, lignin, trehalose, soluble protein, POD, and SOD substantially increased with prolonged stress time. The content of β-amylase was not significantly increased, and that of ABA significantly decreased and then increased.
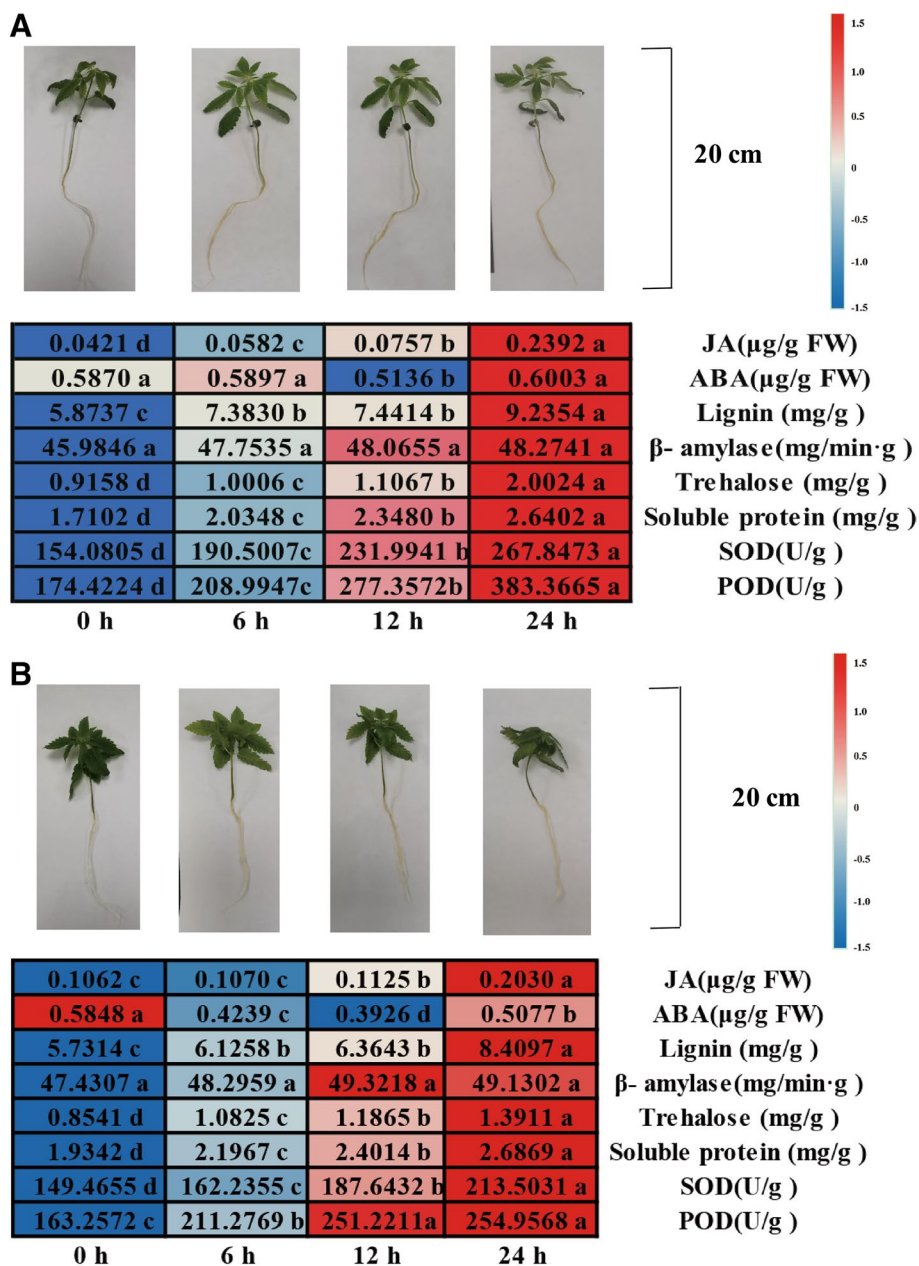

Fig. 1 Morphological and physiochemical changes in industrial hemp under NaHCO₃ stress. **A** The morphological and physiochemical changes in Huoma No. 1 under NaHCO₃ stress; values followed by different lowercase letters represent $p \leq 0.05$. **B** The morphological and physiochemical changes in Jindao-15 under NaHCO₃ stress; values followed by different lowercase letters represent $p \leq 0.05$

Cao *et al. BMC Plant Biology*   (2023) 23:509

Page 4 of 11

Quality analysis of RNA-seq data

The 12 miRNA sequencing libraries were sequenced, and approximately 225.36 M clean reads were obtained. The Q-score at the Q30 level was more than 85%, and the ratio of tagged sequences compared with the known reference genome was between 8.25% and 30.45%. Among the 12 miRNA libraries, 290 miRNAs were obtained, including 4 known and 286 novel miRNAs (Supplementary Table A3). The 12 mRNA libraries were sequenced, and approximately 79.22 Gb clean data were obtained. The Q-score at the Q30 level was more than 93.71%, and the ratio of tagged sequences compared with the known

reference genome was between 73.43% and 80.62% (Supplementary Table A4).

DEGs under NaHCO$_3$ stress

A total of 18,215 mRNAs (Fig. 2A) and 74 miRNAs (Fig. 2B) were identified as differentially expressed under NaHCO$_3$ stress. Additionally, 57.27% of mRNA and 67.57% of miRNA were upregulated, and 42.73% of mRNA and 32.43% of miRNA were downregulated. The mRNA (Fig. 2C) and miRNA (Fig. 2D) expression levels were significantly different in response to NaHCO$_3$ stress in the clustering heatmap.
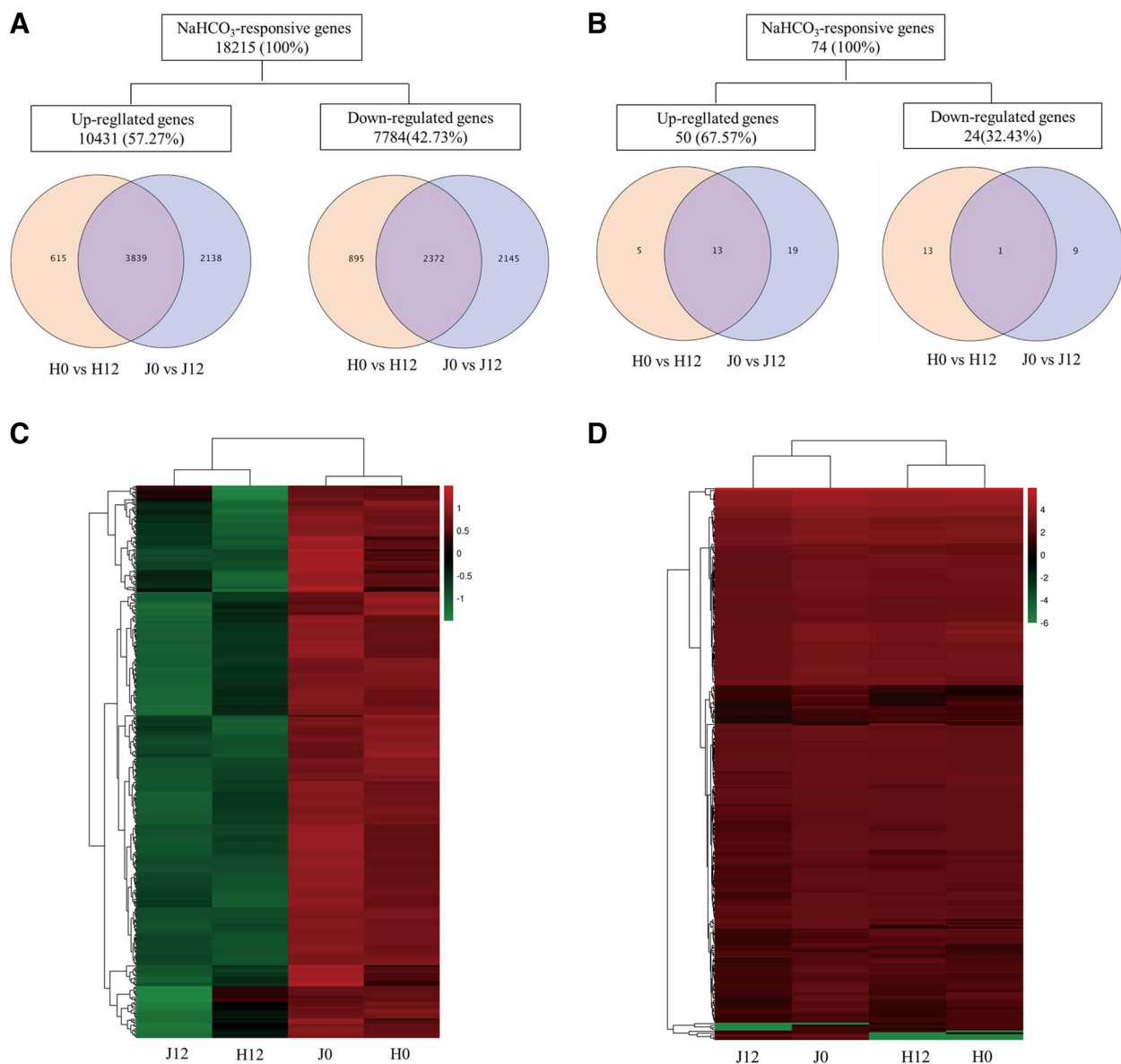

Fig. 2 The expression profile of DEGs in industrial hemp roots under NaHCO$_3$ stress. **A** Number of differentially expressed mRNAs. **B** Number of differentially expressed miRNAs. **C** Heatmap of mRNA expression profiles. **D** Heatmap of miRNA expression profiles

Cao *et al. BMC Plant Biology*   (2023) 23:509

Page 5 of 11

DEGs were classified by Venn diagram. The 1503 and 4267 differentially expressed mRNAs were assigned to 'Huoma No. 1' and 'Jindao-15', respectively. According to the GO enrichment analysis (Fig. 3), these DEGs were abundantly enriched in GO terms including cellular process (GO:0009987), metabolic process (GO:0008152), heterocyclic compound binding (GO:1901363), and organic cyclic compound binding (GO:0097159). The 6218 co-expressed DEGs were enriched in the membrane (GO:0016020), ion binding (GO:0043167), and cellular process (GO:0009987) GO terms.

The KEGG pathway enrichment analysis provided information on pathways of upregulated and downregulated DEGs under NaHCO$_3$ stress (Supplementary materials_2). The upregulated DEGs in Huoma No. 1 were mainly enriched in the peroxisome, endocytosis, and carbon metabolism; however, the downregulated DEGs of Huoma No. 1 were mainly enriched in plant hormone signal transduction, the MAPK signalling pathway, and starch and sucrose metabolism. The upregulated DEGs of Jindao-15 were mainly enriched in plant hormone signal transduction, starch and sucrose metabolism, and protein processing in the endoplasmic reticulum. However, the downregulated DEGs of Jindao-15 were mainly enriched in the ribosome, carbon metabolism, and starch and sucrose metabolism. Furthermore, the upregulated co-expressed DEGs detected under NaHCO$_3$ stress were mainly enriched in plant hormone signal transduction, the MAPK signalling pathway, and carbon metabolism. In contrast, the downregulated co-expressed DEGs were mainly enriched in plant hormone signal transduction, the MAPK signalling pathway, and starch and sucrose metabolism.

Integrated miRNA–mRNA analysis

A targeted regulatory relationship between miRNA and mRNA was visualized using Cytoscape. The network identified 230 miRNA–mRNA interactions involving 16 miRNAs and 179 mRNAs in Huoma No. 1 and Jindao-15 (Fig. 4, Supplementary materials_3). The neighbour-joining phylogenetic tree revealed that novel_miR_179 and novel_miR_75 clustered with cca-miR156 [24], nta-miR156 [25], and gma-miR156 [26] were clustered into one group (Fig. 5); novel_miR_207 and ath-miR827 [27] were clustered into another group; and novel_miR_55 and mtr-miR5260 [28] were clustered into a third group.

qRT–PCR validation of the RNA-seq data

The expression levels of ten mRNAs and two miRNAs related to NaHCO$_3$ stress were selected to validate the reliability of mRNA and miRNA through qRT-PCR. The qRT–PCR results were similar to those of the RNA-seq analysis (Fig. 6).
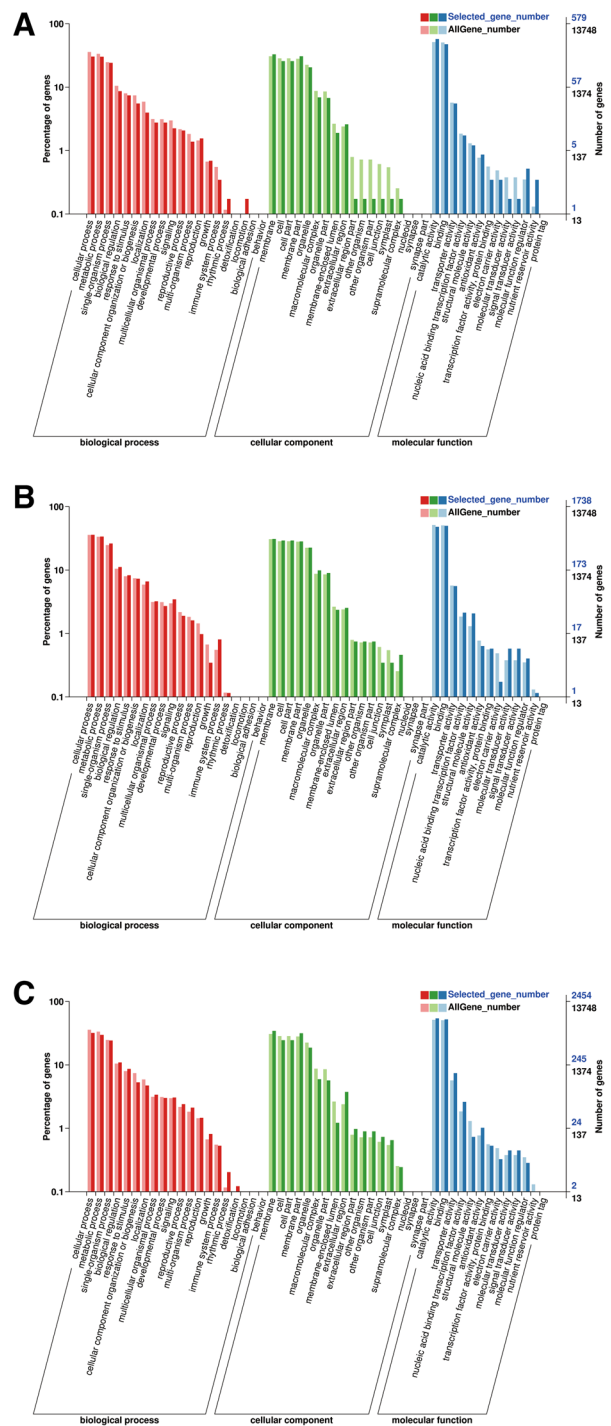

Fig. 3 GO classification of the DEGs. **A** GO classification of DEGs in the (H0_vs_H12)_vs_(J0_vs_J12) group of Huoma No. 1. **B** GO classification of DEGs in the (H0_vs_H12)_vs_(J0_vs_J12) group of JinDao 15. **C** GO classification of co-expressed DEGs in the (H0_vs_H12)_vs_(J0_vs_J12) group
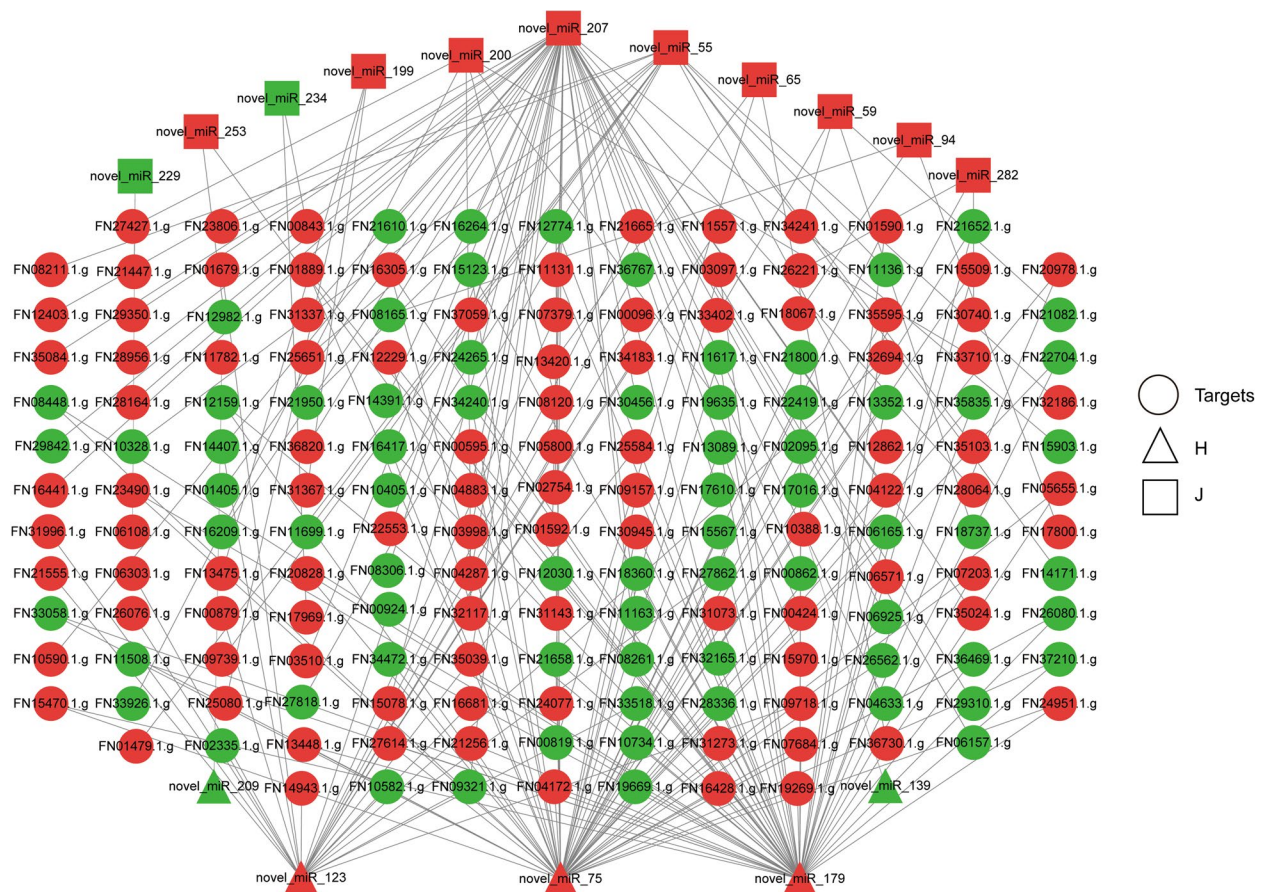
Cao *et al. BMC Plant Biology* (2023) 23:509

Page 6 of 11

Fig. 4 miRNA–mRNA interactions under NaHCO$_3$ stress. The circles are target mRNAs. The triangles and squares are differentially expressed miRNAs of Huoma No. 1 and Jindao-15, respectively. Green and red represent downregulated and upregulated genes, respectively

Discussion

The root morphology, traits, and physio-biochemical characteristics are generally affected by salinity stress [29–31], which hinders the normal growth, development, and biomass of the plant [5]. The inhibition of industrial hemp growth and development by salinity stress varies with the cultivars [32, 33]. This study used the morphology and physio-biochemical characteristics (the contents of phytohormone, lignin, trehalose, soluble protein, peroxidase, and superoxide dismutase) to describe the industrial hemp seedlings before and after NaHCO$_3$ stress. Then, differentially expressed miRNAs and mRNAs in industrial hemp roots under NaHCO$_3$ stress were analysed to explore the potential mechanism. Some significant miRNA-mRNA pairs and their potential roles were identified under NaHCO$_3$ stress. Finally, the differences in physiological and biochemical characteristics before and after NaHCO$_3$ stress in some important pathways were analysed. This paper offers a novel understanding of the response mechanism of other related species to alkali stress.

RNA-seq analysis

Our study focused on the 10,431 upregulated and 7784 downregulated DEGs and the pathways of carbon metabolism, starch and sucrose metabolism, and plant hormone signal transduction. The enrichment of these pathways was consistent with the results of a previous study [15].

miRNAs respond to stress by regulating the gene transcription levels of target mRNAs [17, 18]. Several miRNAs related to salt stress tolerance have been found in *Nicotiana tabacum* [18], *Arabidopsis thaliana*[34], *Medicago truncatula* [35], *Oryza sativa* [36], and *Zea mays* [37]. In this study, a total of 18,215 mRNAs and 74 miRNAs were found to respond to NaHCO$_3$ stress in industrial hemp. We identified significant regulation of the highly conserved miR156 family under NaHCO$_3$ stress. miRNA156 expression increases salt stress tolerance and helps the plant withstand stress conditions until conditions become suitable [34, 38, 39]. The expression of the miR156 family (novel_miR_179 and novel_miR_75) was upregulated after 12 h of NaHCO$_3$ treatment in
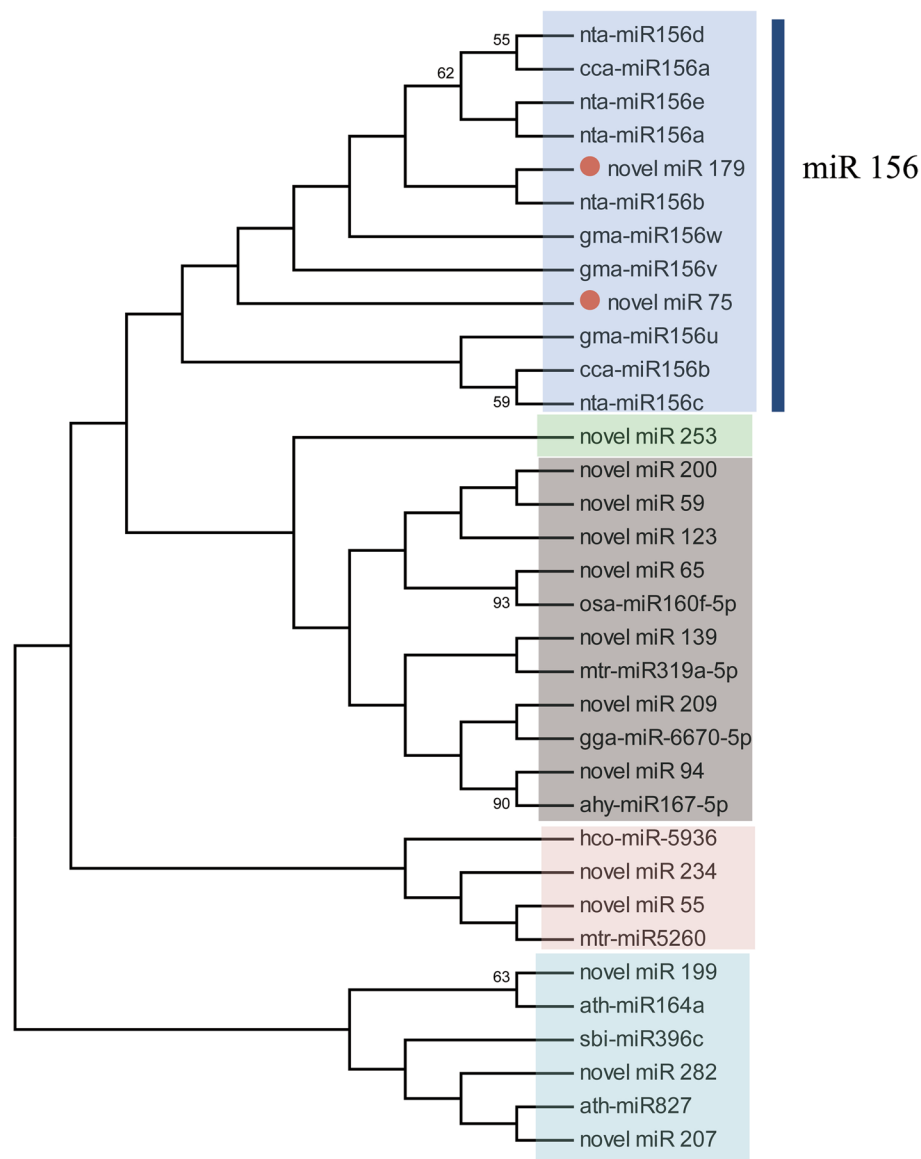
Fig. 5 miRNA clustering using the neighbour-joining method.

the salt–alkali tolerant variety, indicating that NaHCO$_3$ stress induced the expression of novel_miR_179 and novel_miR_75 and improved the adaptability of industrial hemp to the alkaline environment. The targeted regulatory relationship between mRNA and miRNA revealed that *NewGene_9378* (*PRPF 19*), FN20728.1.g (*PRPF 17*), and *NewGene_5122* (*DHX8/PRP22*) were regulated by novel_miR_179 and novel_miR_75, and these genes were annotated in the spliceosome pathway, which is mainly involved in the mRNA surveillance pathway, RNA transport, and spliceosome pathway [34]. Overexpression of HV-MIR827 improves stress tolerance in barley [27],

and MTR-MIR5260 is related to the response of tobacco to biological stress [28]. In this study, novel_miR_207 and novel_miR_55 of the salt stress-sensitive variety were clustered with ATH-MIR827 and MTR-MIR5260, respectively. Hence, we speculated that novel_miR_207 and novel_miR_55 could also improve the salt adaptability of the salt stress-sensitive variety. Furthermore, the expression patterns of these miRNAs were different in the two varieties. Therefore, these differentially expressed miRNAs are helpful for the further study of the response and adaptation mechanism of different varieties of industrial hemp to salt–alkali stress [13, 40].
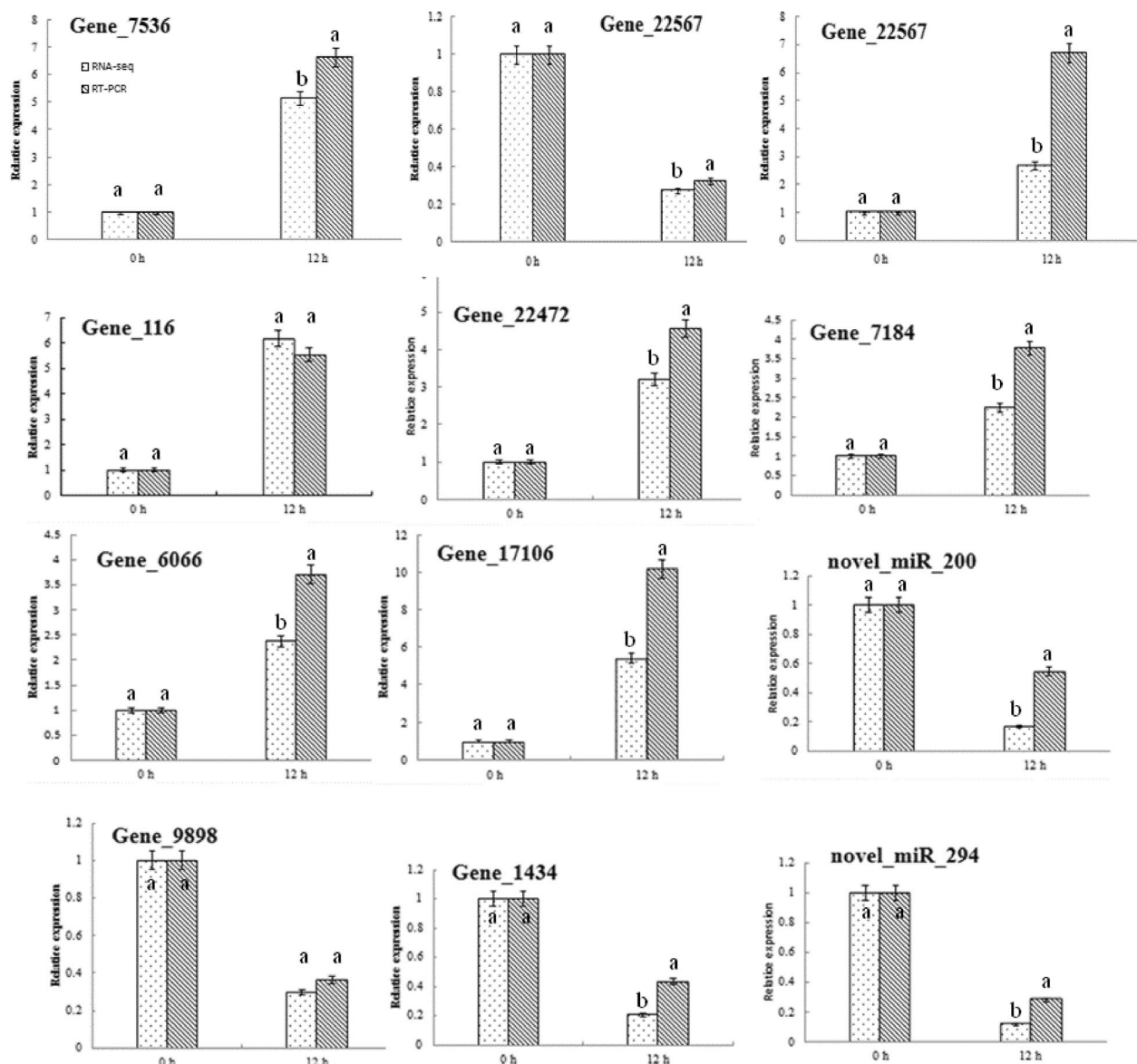
Cao *et al. BMC Plant Biology*   (2023) 23:509

Page 8 of 11

Fig. 6 qRT-PCR analysis of differentially expressed miRNAs and mRNAs in industrial hemp roots under NaHCO$_3$ stress

Plant hormone signal transduction pathway

The regulatory role of hormones is essential under high salt stress [41]. The plant hormone signal transduction pathway revealed that the key hub genes (*new-Gene_13657* and *newGene_11233*) were related to proteins TIFY 6B and phosphatase 2C 8. TIFY positively responds to alkaline stress by the ectopic expression of *GsTIFY10a* and *AtTIFY10a* and *AtTIFY10b* knockout [42]. In this study, *newGene_13657* was upregulated, and JA content was also increased. After 12 h of NaHCO$_3$ stress, *newGene_11233* was upregulated in the salt–alkali-sensitive variety but was normally expressed in the salt–alkali-tolerant variety. Under stress, the PP2C gene

is upregulated and gradually downregulated in maize and Arabidopsis [43, 44], and its expression is negatively correlated with ABA signal transduction [45]. Herein, the ABA content decreased and then gradually increased, and the degree of decrease in the sensitive variety was higher than that in the tolerant variety. However, according to the variation in ABA content in industrial hemp, this gene would also be downregulated after a period of stress. Therefore, it is speculated that after NaHCO$_3$ stress, the TIFY family-related genes were upregulated, and PP2C-related genes were upregulated and then gradually downregulated in industrial hemp roots, inhibiting ABA signalling in the short term, promoting jasmonate

signal transduction, and ultimately regulating the strategies related to NaHCO₃ stress.

Starch and sucrose metabolism and carbon metabolism pathways

Starch and sucrose metabolism, a stress response, mediates plant responses to abiotic stresses [46, 47]. The starch and sucrose metabolism pathway revealed that the key hub genes *(newGene_2736* and *newGene_5139)* were related to glucan endo-1,3-β-glucosidase 1 and β-amylase 3 [48, 49]. The expression of the β-glucosidase and β-amylase-related genes was upregulated in industrial hemp roots after NaHCO₃ stress. However, the expression of the β-glucosidase gene was normal in the salt–alkali-sensitive variety. The PPI of the carbon metabolism pathway revealed that the key hub gene *(newGene_1914)* was related to 3-hydroxybutyryl-CoA dehydrogenase[50]. The expression of *newGene_1914* was gradually upregulated in the salt–alkali-tolerant variety and downregulated in the sensitive variety. Relatively low starch content is typically characteristic of tissues undergoing rapid growth, and 3-hydroxybutyryl-CoA dehydrogenase maintains

root meristem activity [50–52]. With prolonged NaHCO₃ stress, β-amylase activity increased; especially 24 h after NaHCO₃ stress, the β-amylase activity of the tolerant variety increased by 5.0%, and that of the sensitive variety increased by 3.6%. Previous studies have shown that the root biomass of the salt–alkali tolerant variety was greater than that of the sensitive variety under NaHCO₃ stress, indicating that the difference in starch decomposability in the roots is responsible for the different salt tolerance of industrial hemp [13].

Conclusions

The miRNA and mRNA profiles of industrial hemp under NaHCO₃ stress were comprehensively analysed. Overall, 18,215 mRNAs and 74 miRNAs were identified as differentially expressed in response to NaHCO₃ stress. The common DEGs revealed that industrial hemp utilizes similar strategies, such as membrane, ion binding, and cellular processes, to respond to NaHCO₃ stress. However, many essential biological processes, including endocytosis, plant hormone signal transduction, and starch and sucrose metabolism, were
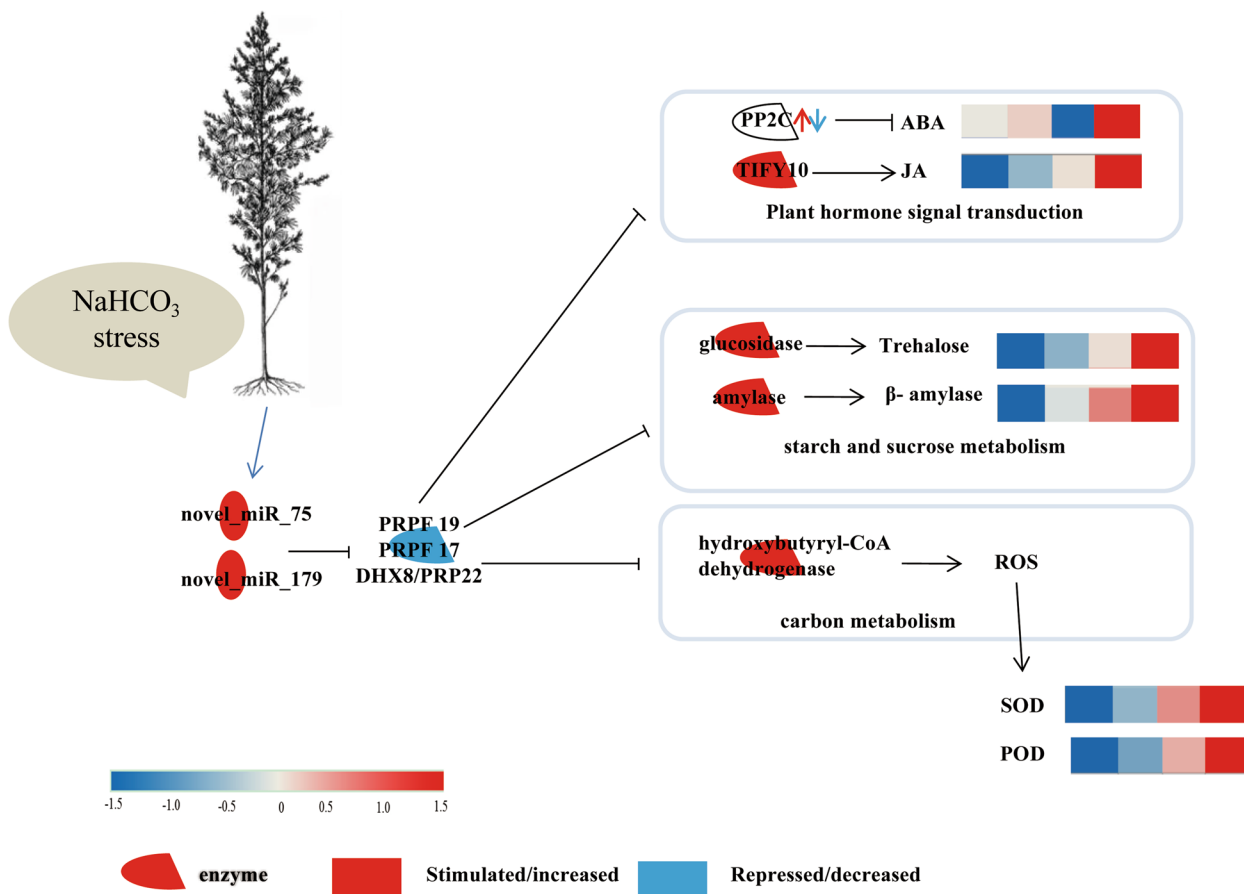

Fig. 7 Important pathways in the response to NaHCO3 stress in industrial hemp

Cao *et al. BMC Plant Biology*   (2023) 23:509

Page 10 of 11

specifically enriched according to GO and KEGG pathway analysis under NaHCO$_3$ stress. Starch and sucrose metabolism, carbon metabolism, plant hormone signal transduction, and the spliceosome were important pathways in the NaHCO$_3$ stress response in industrial hemp. In addition, some novel miRNAs from the miR156 family with their target transcript genes were predicted as ideal candidates for future manipulation to improve NaHCO$_3$ stress tolerance (Fig. 7). In summary, these findings provide a better understanding of the industrial hemp response to alkali stress at the miRNA and mRNA levels and provide candidate miRNAs and mRNAs for resistance breeding.

Supplementary Information

The online version contains supplementary material available at https://doi.org/10.1186/s12870-023-04463-w.

Additional file 1: Table A2. List of primer sequences used in this study.

Additional file 2: Table A3. The quality of miRNA sequence data in three replicates for all samples.

Additional file 3: Table A4. The quality of mRNA sequence data in three replicates for all samples.

Additional file 4: Supplementary materials_2. The KEGG pathway enrichment analysis.

Additional file 5: Supplementary materials_3. The network of miRNA–mRNA interactions involving 16 miRNAs and 179 mRNAs among Huoma No. 1 and Jindao-15.

Additional file 6: Table A1. Quality of RNA samples used in this study

Declarations

Ethics approval and consent to participate
Experimental research and field studies on industrial hemp, including the collection of plant material, comply with relevant institutional, national, and international guidelines and legislation. The Huoma No. 1 seeds are certified by the Crop Variety Examination and Approval Committee of Heilongjiang Province, China, under the reference 2015005. The seeds of Huoma No. 1 were supplied by the Daqing Branch of Heilongjiang Academy of Sciences, China. The Jindao-15 seeds were registered by Ukrainian National Seed Registry Department and Jindao-15 was produced in the Ukrainian Academy of Agricultural Sciences in 2014. The tetrahydrocannabinol contents of Huoma No. 1 and Jindao-15 are not exceeded 0.3%, in accordance with National Standard NY/T3252.1—2018 of the People's Republic of China.

Consent for publication
Not applicable.

Competing interests
Authors declare that they have no conflict of interest for the publication of the manuscript.

References

1. Manaia JP, Manaia AT, Rodriges L. Industrial hemp fibers: an overview. Fibers. 2019;7(12):106.
2. Hu H, Liu H, Liu F. Seed germination of hemp (*Cannabis sativa* L.) cultivars responds differently to the stress of salt type and concentration. Ind Crops Products. 2018;123:254–61.
3. Zhao H, Xiong H, Chen J. Regional comparison and strategy recommendations of industrial hemp in China based on a SWOT analysis. Sustainability. 2021;13(11):6419.
4. Wang Y, Wang J, Guo D, Zhang H, Che Y, Li Y, Tian B, Wang Z, Sun G, Zhang H. Physiological and comparative transcriptome analysis of leaf response and physiological adaption to saline alkali stress across pH values in alfalfa (*Medicago sativa*). Plant Physiol Biochem. 2021;167:140–52.
5. Fang S, Hou X, Liang X. Response Mechanisms of plants under saline-alkali stress. Front Plant Sci. 2021;12:1049.
6. An Y, Gao Y, Tong S, Liu B. Morphological and physiological traits related to the response and adaption of Bolboschoenus planiculmis seedlings grown under salt-alkaline stress conditions. Front Plant Sci. 2021;12:307.
7. Deng C, Zhang G, Pan X, Zhao K. Chlorophyll fluorescence and gas exchange responses of maize seedlings to saline-alkaline stress. Bulgarian J Agric Sci. 2010;16(1):49–58.
8. Abdel Latef AA, Tran LSP. Impacts of priming with silicon on the growth and tolerance of maize plants to alkaline stress. Front Plant Sci. 2016;7:243.
9. Du B, Zhao W, An Y, Li Y, Zhang X, Song L, Guo C. Overexpression of an alfalfa glutathione S-transferase gene improved the saline-alkali tolerance of transgenic tobacco. Biol Open. 2019;8(9):bio043505.
10. Ye X, Wang H, Cao X, Jin X, Cui F, Bu Y, Liu H, Wu W, Takano T, Liu S. Transcriptome profiling of Puccinellia tenuiflora during seed germination under a long-term saline-alkali stress. BMC genomics. 2019;20(1):1–17.
11. Wu J, Zhang J, Li X, Liu J, Niu Z, Wang L. An overexpression of the *AP2/ERF* transcription factor from Iris typhifolia in Arabidopsis thaliana confers tolerance to salt stress. Biologia Plantarum. 2019;63(1):776–84.
12. An D, Chen JG, Gao YQ, Li X, Chao ZF, Chen ZR, Li QQ, Han ML, Wang YL, Wang YF. *AtHKT1* drives adaptation of Arabidopsis thaliana to salinity by reducing floral sodium content. PLoS Genetics. 2017;13(10).
13. Hu H, Liu H, Du G, Fei Y, Deng G, Yang Y, Feihu L. Fiber and seed type of hemp (*Cannabis sativa* L.) responded differently to salt-alkali stress in seedling growth and physiological indices. Industrial Crops Prod. 2019;129:624–30.
14. Cheng X, Deng G, Su Y, Liu JJ, Yang Y, Du GH, Chen ZY, Liu FH. Protein mechanisms in response to NaCl-stress of salt-tolerant and salt-sensitive industrial hemp based on iTRAQ technology. Industrial Crops Prod. 2016;83:444–52.
15. Cao K, Sun Y, Han C, Zhang X, Zhao Y, Jiang Y, Jiang Y, Sun X, Guo Y, Wang X. The transcriptome of saline-alkaline resistant industrial hemp (*Cannabis sativa* L.) exposed to NaHCO$_3$ stress. Industrial Crops Prod. 2021;170:113766.
16. Hasan MA, Hussain MH, Chowdhury AS, Dhar SB, Abedin M, Fima IN. Computational identification of potential microRNAs and their targets from expressed sequence tags of marijuana (*Cannabis sativa*). Meta Gene. 2016;10:45–55.

Cao *et al. BMC Plant Biology*   (2023) 23:509

Page 11 of 11

17. Sharma N, Tripathi A, Sanan-Mishra N. Profiling the expression domains of a rice-specific microRNA under stress. Front Plant Sci. 2015;6:333.

18. Xu J, Chen Q, Liu P, Jia W, Chen Z, Xu Z. Integration of mRNA and miRNA analysis reveals the molecular mechanism underlying salt and alkali stress tolerance in tobacco. Int J Mol Sci. 2019;20(10):2391.

19. Wani SH, Kumar V, Khare T, Tripathi P, Shah T, Ramakrishna C, Aglawe S, Mangrauthia SK. miRNA applications for engineering abiotic stress tolerance in plants. Biologia. 2020;75(7):1063–81.

20. Kanehisa M, Furumichi M, Sato Y, Kawashima M, Ishiguro-Watanabe M. KEGG for taxonomy-based analysis of pathways and genomes. Nucleic Acids Res. 2023;51(D1):D587–92.

21. Gao K, Wang Z, Qiu X, Song J, Wang H, Zhao C, Wang X, Chang Y. Transcriptome analysis of body wall reveals growth difference between the largest and smallest individuals in the pure and hybrid populations of *Apostichopus japonicus*. Comp Biochem Physiol Part D Genomics Proteomics. 2019;31. https://doi.org/10.3390/ijms21134615

22. Kong W, Zhang C, Qiang Y, Zhong H, Zhao G, Li Y. Integrated RNA-seq analysis and Meta-QTLs mapping provide insights into cold stress response in rice seedling roots. Int J Mol Sci. 2020;21(13):4615.

23. Livak KJ, Schmittgen TD. Analysis of relative gene expression data using real-time quantitative PCR and the $2^{-\Delta\Delta CT}$ method. Methods. 2001;25(4):402–8.

24. De Paola D, Cattonaro F, Pignone D, Sonnante G. The miRNAome of globe artichoke: conserved and novel micro RNAs and target analysis. BMC Genomics. 2012;13(1):1–14.

25. Tang S, Wang Y, Li Z, Gui Y, Xiao B, Xie J, Zhu Q-H, Fan L. Identification of wounding and topping responsive small RNAs in tobacco (*Nicotiana tabacum*). BMC Plant Biol. 2012;12(1):1–16.

26. Turner M, Yu O, Subramanian S. Genome organization and characteristics of soybean microRNAs. BMC Genomics. 2012;13(1):1–16.

27. Ferdous J, Whitford R, Nguyen M, Brien C, Langridge P, Tricker PJ. Drought-inducible expression of Hv-miR827 enhances drought tolerance in transgenic barley. Funct Integr Genomics. 2017;17(2):279–92.

28. Pradhan M, Pandey P, Baldwin IT, Pandey SP. Argonaute4 modulates resistance to fusarium brachygibbosum infection by regulating jasmonic acid signaling. Plant Physiol. 2020;184(2):1128–52.

29. Arif MR, Islam MT, Robin AHK. Salinity stress alters root morphology and root hair traits in Brassica napus. Plants. 2019;8(7):192.

30. Postnikova OA, Shao J, Nemchinov LG. Analysis of the alfalfa root transcriptome in response to salinity stress. Plant Cell Physiol. 2013;54(7):1041–55.

31. Neumann PM. Inhibition of root growth by salinity stress: toxicity or an adaptive biophysical response? In: Structure and function of roots. Springer Netherlands; 1995:299–304.

32. Hu L, Zhang P, Jiang Y, Fu J. Metabolomic analysis revealed differential adaptation to salinity and alkalinity stress in Kentucky bluegrass (*Poa pratensis*). Plant Mol Biol Rep. 2015;33(1):56–68.

33. Liu J, Qiao Q, Cheng X, Du G, Deng G, Zhao M, Liu F. Transcriptome differences between fiber-type and seed-type *Cannabis sativa* variety exposed to salinity. Physiol Mol Biol Plants Int J Function Plant Biol. 2016;22(4):429–43.

34. Cui LG, Shan JX, Shi M, Gao JP, Lin HX. The miR156-SPL 9-DFR pathway coordinates the relationship between development and abiotic stress tolerance in plants. Plant J. 2014;80(6):1108–17.

35. Cao C, Long R, Zhang T, Kang J, Wang Z, Wang P, Sun H, Yu J, Yang Q. Genome-wide identification of microRNAs in response to salt/alkali stress in Medicago truncatula through high-throughput sequencing. Int J Mol Sci. 2018;19(12):4076.

36. Parmar S, Gharat SA, Tagirasa R, Chandra T, Behera L, Dash SK, Shaw BP. Identification and expression analysis of miRNAs and elucidation of their role in salt tolerance in rice varieties susceptible and tolerant to salinity. PloS One. 2020;15(4): e0230958.

37. Fu R, Zhang M, Zhao Y, He X, Ding C, Wang S, Feng Y, Song X, Li P, Wang B. Identification of salt tolerance-related microRNAs and their targets in maize (*Zea mays* L.) using high-throughput sequencing and degradome analysis. Front Plant Sci 2017;8:864.

38. Kang T, Yu CY, Liu Y, Song WM, Bao Y, Guo XT, Li B, Zhang HX. Subtly manipulated expression of ZmmiR156 in tobacco improves drought and salt tolerance without changing the architecture of transgenic plants. Front Plant Sci. 2020;10:1664.

39. Xu T, Zhang L, Yang Z, Wei Y, Dong T. Identification and functional characterization of plant MiRNA under salt stress shed light on salinity resistance improvement through MiRNA manipulation in crops. Front Plant Sci. 2021;12:972.

40. Yin Z, Li Y, Yu J, Liu Y, Li C, Han X, Shen F. Difference in miRNA expression profiles between two cotton cultivars with distinct salt sensitivity. Mol Biol Reports. 2012;39(4):4961–70.

41. Yue Y, Wang J, Ren W, Zhou Z, Long X, Gao X, Rengel Z. Expression of genes related to plant hormone signal transduction in Jerusalem Artichoke (*Helianthus tuberosus* L.) seedlings under salt stress. Agronomy. 2022;12(1):163.

42. Zhu D, Li R, Liu X, Sun M, Wu J, Zhang N, Zhu Y. The positive regulatory roles of the *TIFY10* proteins in plant responses to alkaline stress. PloS One. 2014;9(11): e111984.

43. Liu X, Zhu Y, Zhai H, Cai H, Ji W, Luo X, Li J, Bai X. AtPP2CG1, a protein phosphatase 2C, positively regulates salt tolerance of Arabidopsis in abscisic acid-dependent manner. Biochem Biophys Res Commun. 2012;422(4):710–5.

44. Li FH, Fu FL, Sha LN, He L, Li WC. Differential expression of serine/threonine protein phosphatase type-2C under drought stress in maize. Plant Mol Biol Report. 2009;27(1):29–37.

45. Kang Y, Yang X, Liu Y, Shi M, Zhang W, Fan Y, Yao Y, Zhang J, Qin S. Integration of mRNA and miRNA analysis reveals the molecular mechanism of potato (*Solanum tuberosum* L.) response to alkali stress. Int J Biol Macromol. 2021;182:938–49.

46. Ruan YL. Sucrose metabolism: gateway to diverse carbon use and sugar signaling. Ann Rev Plant Biol. 2014;65:33–67.

47. Thalmann M, Santelia D. Starch as a determinant of plant fitness under abiotic stress. New Phytologist. 2017;214(3):943–51.

48. Zhu H, Yang X, Wang X, Li Q, Guo J, Ma T, Zhao C, Tang Y, Qiao L, Wang J. The sweetpotato β-amylase gene IbBAM1.1 enhances drought and salt stress resistance by regulating ROS homeostasis and osmotic balance. Plant Physiol Biochem. 2021;168:167–76.

49. Baba SA, Vishwakarma RA, Ashraf N. Functional characterization of *CsBGlu12*, a β-glucosidase from Crocus sativus, provides insights into its role in abiotic stress through accumulation of antioxidant flavonols. J Biol Chem. 2017;292(11):4700–13.

50. Xu L, Zhao H, Ruan W, Deng M, Wang F, Peng J, Luo J, Chen Z, Yi K. Abnormal inflorescence meristen1 functions in salicylic acid biosynthesis to maintain proper reactive oxygen species levels for root meristem activity in rice. Plant Cell. 2017;29(3):560–74.

51. Purdy SJ, Maddison AL, Cunniff J, Donnison I, Clifton-Brown J. Non-structural carbohydrate profiles and ratios between soluble sugars and starch serve as indicators of productivity for a bioenergy grass. AoB Plants. 2015;7:plv032.

52. Dong S, Beckles DM. Dynamic changes in the starch-sugar interconversion within plant source and sink tissues promote a better abiotic stress response. J Plant Physiol. 2019;234:80–93.

Publisher's Note

Springer Nature remains neutral with regard to jurisdictional claims in published maps and institutional affiliations.